Title

Thermodynamic response of soft biological tissues to pulsed infrared-laser irradiation

Journal

Biophysical Journal, 70(6)

ISSN

0006-3495

Authors

Venugopalan, V
Nishioka, NS
Mikić, BB

Publication Date

1996-06-01

DOI

10.1016/s0006-3495(96)79868-5

Thermodynamic Response of Soft Biological Tissues to Pulsed Infrared-Laser Irradiation

V. Venugopalan,*‡ N. S. Nishioka,* and B. B. Mikić‡
*Wellman Laboratories of Photomedicine, Harvard Medical School, Massachusetts General Hospital, Boston, Massachusetts 02114, and ‡Department of Mechanical Engineering, Massachusetts Institute of Technology, Cambridge, Massachusetts 02139 USA

ABSTRACT The physical mechanisms that achieve tissue removal through the delivery of short pulses of high-intensity infrared laser radiation, in a process known as laser ablation, remain obscure. The thermodynamic response of biological tissue to pulsed infrared laser irradiation was investigated by measuring and analyzing the stress transients generated by Q-sw Er:YSGG (λ = 2.79 μm) and TEA CO_2 (λ = 10.6 μm) laser irradiation of porcine dermis using thin-film piezoelectric transducers. For radiant exposures that do not produce material removal, the stress transients are consistent with thermal expansion of the tissue samples. The temporal structure of the stress transients generated at the threshold radiant exposure for ablation indicates that the onset of material removal is delayed with respect to irradiation. Once material removal is achieved, the magnitude of the peak compressive stress and its variation with radiant exposure are consistent with a model that considers this process as an explosive event occurring after the laser pulse. This mechanism is different from ArF- and KrF-excimer laser ablation where absorption of ultraviolet radiation by the collagenous tissue matrix leads to tissue decomposition during irradiation and results in material removal via rapid surface vaporization. It appears that under the conditions examined in this study, explosive boiling of tissue water is the process that mediates the ablation event. This study provides evidence that the dynamics and mechanism of tissue ablation processes can be altered by targeting tissue water rather than the tissue structural matrix.

GLOSSARY

A	area (m^2)
c_a	propagation speed of a longitudinal acoustic wave ($m\ s^{-1}$)
c_i	propagation speed of a longitudinal acoustic wave in region i, i being an integer ($m\ s^{-1}$)
c_p	specific heat at constant pressure ($J\ kg^{-1}\ K^{-1}$)
c_v	specific heat at constant volume ($J\ kg^{-1}\ K^{-1}$)
C	capacitance (F)
e_{33}	piezoelectric stress constant for axial compression ($N\ C^{-1}$)
Fo	Fourier number of the laser pulse duration relative to the characteristic optical absorption depth within the tissue ($\equiv \alpha\mu_a^2 t_p$)
Fo_δ	Fourier number of the laser pulse duration relative to the characteristic size of the tissue chromophore ($\equiv \alpha t_p/\delta^2$)
h_{fg}	latent heat of vaporization ($J\ kg^{-1}$)
I''	linear momentum per unit area ($kg\ m^{-1}\ s^{-1}$)
m''	mass removal per unit area ($kg\ m^{-2}$)
$\mathcal{O}(x)$	order of magnitude of x
p	pressure (Pa)
p_i	pressure in region i, i being an integer (Pa)
q_0''	incident laser irradiance ($W\ m^{-2}$)
q_0'''	incident volumetric power density ($W\ m^{-3}$)
R	bubble radius (m)
t	time (s)
t_p	laser pulse duration (s)
T	temperature (K)
u_i	velocity in region i, i being an integer ($m\ s^{-1}$)
V	voltage (V) or volume (m^3)
x	axial position (m) or volume fraction

Greek symbols

α	thermal diffusivity ($m^2\ s^{-1}$)
δ	characteristic size of the tissue chromophore (m)
δ_{etch}	depth of material removal achieved by ablation (m)
ϵ_0''	incident radiant exposure ($J\ m^{-2}$)
ϵ_{th}''	threshold radiant exposure at which bulk material removal is achieved ($J\ m^{-2}$)
ϵ'''	volumetric energy density ($J\ m^{-3}$)
ϵ_{th}'''	threshold volumetric energy density at which bulk material removal is achieved ($J\ m^{-3}$)
η	ratio of incident radiant exposure to threshold radiant exposure ($\equiv \epsilon_0''/\epsilon_{th}''$)
γ_i	ratio of specific heats ($\equiv c_p/c_v$) in region i
λ	laser wavelength (m)
Λ	multiplicative constant used in the scaling law for rapid surface vaporization ($kg^{1/3}\ m^{-1}\ s^{-2/3}$)
μ_a	optical absorption coefficient of incident radiation (m^{-1})
Ω	density of nucleation centers (m^{-3})

Received for publication 22 September 1995 and in final form 16 February 1996.

Address reprint requests to Dr. Vasan Venugopalan, Lewis Thomas Laboratory, Departments of Molecular Biology and Physics, Princeton University, Princeton, NJ 08544. Tel.: 609-258-3479; Fax: 609-258-6175; E-mail: vasan@phoenix.princeton.edu.

0006-3495/96/06/2981/13 $2.00

ρ	material density (kg m^{-3})
σ	stress (Pa)
σ_p	peak compressive stress (Pa)
τ_m	dimensionless mechanical equilibration time ($\equiv \mu_a c_a t_p$)
Υ	multiplicative constant used in the scaling law for explosive material removal

Subscripts

f	fluid or liquid
sat	saturation conditions
sp	spinodal conditions
v	vapor
∞	conditions in the surroundings

INTRODUCTION AND MOTIVATION

The widespread use of infrared (IR) lasers for biomedical applications is based largely on the fact that water, the chief constituent of most soft biological tissues, strongly absorbs optical radiation in the IR region. By choosing appropriate IR wavelengths one can produce a range of tissue effects from deep coagulation using Nd:YAG lasers operating at λ = 1.064 μm to very clean and precise cutting using Q-switched (Q-sw) Er:YAG/YSGG lasers operating at λ = 2.94 and 2.79 μm. In the mid-1980s, the availability of pulsed CO_2 and solid-state IR lasers for biomedical use generated interest in the efficiency of tissue removal and spatial confinement of thermal injury (Wolbarsht, 1984; Walsh et al., 1988; Walsh and Deutsch, 1989; Ren et al., 1992). Furthermore, as IR lasers are easier to use and maintain than ultraviolet (UV) laser sources and emit radiation with pulse durations and small-signal absorption coefficients in tissue that are comparable to those of UV lasers, the tissue effect produced by pulsed CO_2 and Q-sw Er:YAG/YSGG lasers relative to KrF- and ArF-excimer lasers has been of particular interest. However, these studies revealed that the tissue effects produced by UV and IR laser irradiation are, in fact, quite disparate.

The differences in the tissue effects produced by UV and IR laser ablation are significant. UV lasers cut tissue cleanly with minimal evidence of gross thermal or mechanical injury (Lane et al., 1985; Puliafito et al., 1987), whereas IR lasers typically produce lesions with much thermal injury and macroscopic tissue tearing (Cummings and Walsh, 1993b). For example, the optical penetration depths of KrF-excimer and CO_2 laser radiation in tissue are comparable, at 30 μm and 20 μm, respectively (Walsh and Deutsch, 1988; Dyer and Al-Dhahir, 1990). However, KrF-excimer laser ablation of dermis in vitro results in a zone of thermal injury of less than 5 μm (Lane et al., 1985), whereas CO_2 laser ablation results in at least 50 μm of thermal injury (Walsh et al., 1988; Venugopalan et al., 1991). Similarly, for ArF-excimer laser ablation, an optical penetration depth of 4 μm results in thermal injury only 0.3 μm in extent (Puliafito et al., 1987), whereas for Q-sw Er:YAG/YSGG laser ablation, an optical penetration depth in tissue of ~1–3 μm results in 2–4 μm of thermal injury (Ren et al., 1992).

Many investigators have postulated that these differences in resulting tissue effects are due to distinct ablation mechanisms or to nonlinear tissue optical properties (Srinivasan, 1986; Cummings and Walsh, 1993a; Ediger et al., 1993; Ediger et al., 1994). This has led to much speculation regarding the mechanism of UV laser ablation, with some advocating a novel photochemical process (Srinivasan et al., 1987; Hahn et al., 1995) operative only at UV wavelengths. However, others have maintained that photochemical processes need not be invoked and that the tissue morphology resulting from UV laser ablation is consistent with a removal process that acts via a combination of photothermal and photomechanical mechanisms (Lane et al., 1987; Kitai et al., 1991). Our previous work, which examined the dynamics of ArF- and KrF-excimer laser irradiation of porcine dermis, demonstrated that photothermal and photomechanical mechanisms are sufficient to explain both the dynamics of UV excimer-laser ablation processes and the resulting tissue morphology (Venugopalan et al., 1995).

The possibility that the energy densities achieved within tissue during ablation induce processes that alter the optical absorption of tissue during irradiation has also been investigated. These effects have been shown to be present in Q-sw Er:YAG/YSGG laser ablation of tissue, where the temperature increase induced by laser heating changes the hydrogen bonding structure of tissue water and causes tissue to become more transparent (Cummings and Walsh, 1993a; Walsh and Cummings, 1994). However, this dynamic change in optical properties is significant only at radiant exposures $\gtrsim$200 and 30,000 J m^{-2} for Q-sw Er:YAG and Er:YSGG laser irradiation, respectively (Venugopalan, unpublished calculation). For UV laser ablation, recent studies have shown that 193-nm irradiation of hydrated corneal collagen induces a transient decrease in transmission during an ablative nanosecond laser pulse (Ediger et al., 1993; Ediger et al., 1994), implying that the optical absorption of collagen-based tissues increases during UV irradiation. This result is consistent with preliminary data indicating that the absorption of water at 193 nm increases substantially at higher temperatures (Walsh and Staveteig, 1995). However, the magnitude of this effect has not been quantified, and its ramifications for the ablation process remain unknown. Thus it is unclear whether the observed differences in tissue morphology produced by UV and IR laser ablation result from differences in ablation mechanism, optical penetration depth, or some other undetermined factor.

The goal of this study was to better understand the mechanisms of tissue removal and the resulting tissue morphology by examining the thermodynamic response of soft biological tissues to pulsed IR laser irradiation. This study was motivated by several hypotheses. First, we postulated that the dominant tissue chromophore and its characteristic pathways of decomposition are important factors in determining the mechanism and dynamics of the ablation process

if the following conditions are satisfied:

1. The laser pulse duration t_p is small relative to the characteristic thermal diffusion time across the optical penetration depth $1/\alpha\mu_a^2$, that is, when $\mathrm{Fo} \equiv \alpha\mu_a^2 t_p \leq \mathbb{O}(1)$, where α and μ_a^{-1} are thermal diffusivity of the tissue and the characteristic optical penetration depth of the laser radiation (scattering is assumed negligible), respectively.
2. The laser pulse duration t_p is small relative to the characteristic thermal diffusion time across the characteristic length scale of the chromophore δ^2/α. That is, when $\mathrm{Fo}_\delta \equiv \alpha t_p/\delta^2 \leq \mathbb{O}(1)$, where δ is the characteristic size of the tissue chromophore.

Under these conditions, the energy absorbed by the chromophore is not transported via diffusion to neighboring structures during irradiation. Thus, selective photothermolysis (Anderson and Parrish, 1983) of the chromophore is a potential mechanism for laser ablation. If the chromophore is the tissue structural matrix, the mechanical integrity of the tissue is directly targeted and may result in the breaking of structural bonds to allow material removal. In contrast, if the chromophore does not play an active role in preserving the mechanical integrity of tissue, the dynamics of material removal should be quite different. In IR laser ablation of tissue, water is usually the dominant chromophore and the structural matrix of the tissue is not targeted directly. In this case the characteristic size of the chromophore δ is governed by the size of water-filled spaces within the tissue. For porcine reticular dermis, the tissue used in this study, these spaces correspond to those between the collagen fibers, which have a dimension on order of the fiber diameters, between 1 and 3 μm. To achieve material removal the heated water must expand, to first strain and then fracture the matrix components. This would lead to a slower, albeit more explosive, dynamic process. As such, a fundamental change in ablation mechanism could be affected by simply changing the tissue chromophore without changing parameters that would alter the thermal and mechanical transients generated on the macroscopic scale. This change in ablation mechanism could affect the resulting tissue morphology. There is circumstantial evidence to support this hypothesis. A recent study by Edwards and co-workers provided evidence that tissue ablation using 6.45-μm laser radiation achieves material removal through a mechanism mediated in part by modification of tissue collagen rather than through exclusive heating of water, as is the case for most other IR ablation processes (Edwards et al., 1994). They hypothesized that this was due to combined amide II and water absorption at this wavelength. However, time-resolved data, which would confirm the existence of a different ablation mechanism, are still lacking.

Second, we postulated that the contribution of photomechanical mechanisms to material removal are significant only when the magnitude of laser-induced stresses is sufficient to produce mechanical fracture. As suggested by Albagli and co-workers (Albagli et al., 1994b), a mechanical mechanism for material removal should be energetically more efficient than vaporization, because every bond in the ablated mass need not be broken for material fracture. The contribution of photomechanical mechanisms to material removal should become significant when the stresses generated at the threshold radiant exposure for material removal approach the ultimate tensile strength of the target. This is likely to occur when the laser pulse duration t_p becomes shorter or comparable to the mechanical equilibration time of the heated volume. In a one-dimensional planar geometry this occurs when the dimensionless mechanical equilibration time of the heated layer $\tau_m \equiv \mu_a c_a t_p \leq \mathbb{O}(1)$, where c_a is the speed of longitudinal wave propagation in the medium.

Third, we postulated that the temporal structure of stress transients induced by laser irradiation and the variation in stress amplitude with radiant exposure allow differentiation between photomechanical and photothermal mechanisms for material removal. In this study the thermodynamic response of porcine reticular dermis to exposure of nanosecond pulses of 2.79- and 10.6-μm radiation was measured in vitro. At both wavelengths tissue water is the dominant chromophore (Yannas, 1972; Downing and Williams, 1975). Because of the common chromophore, ablation at these two wavelengths should bear some similarity and the potential role of photomechanical processes can be investigated, because mechanical equilibration of the heated tissue is fully permitted during 2.79-μm irradiation, whereas for 10.6-μm irradiation it is not.

MATERIALS AND METHODS

Thin sections (~400 μm thick) of porcine reticular dermis were prepared using a pneumatic vibrating dermatome (Zimmer, Concord, MA) from tissue acquired immediately postmortem. Samples were kept refrigerated and hydrated in saline (Baxter Healthcare Corp., Deerfield, IL) until use. Sections were irradiated within 24 h of acquisition with pulses generated by an Er:YSGG laser (Schwartz Electro Optics, 1–2-3, Orlando, FL) with a rotating mirror Q-switch or a N_2-starved TEA (transverse excitation at atmospheric pressure) CO_2 laser (model 103; Lumonics, Kanata, Canada). The specific laser and tissue parameters and the characteristic time scales of the laser-tissue interaction are summarized in Table 1.

The active element of the stress transducer was a 9-μm-thick film of piezoelectric polyvinylidene fluoride (PVDF) film with 60-nm-thick alu-

TABLE 1 Relevant laser parameters and dimensionless time scales for TEA CO_2 and Q-sw Er:YSGG laser irradiation of porcine dermis

Laser	λ (nm)	t_p (ns)	μ_a^{-1} (μm)	τ_m ($\equiv \mu_a c_a t_p$)	Fo ($\equiv \alpha\mu_a^2 t_p$)	Fo_δ* ($\equiv \alpha t_p/\delta^2$)
TEA CO_2	10600	30	18‡	2.5	1.2×10^{-5}	$0.4–3 \times 10^{-2}$
Q-sw Er:YSGG	2790	40	3§	20	5.8×10^{-4}	$0.5–5 \times 10^{-2}$

*δ for water is taken as the characteristic fibril diameters in the reticular dermis, which vary between 1 and 3 μm. This is done because the collagen fibrils in the reticular dermis are separated by roughly the same dimension as their diameters (Smith et al., 1982).

‡Using value of μ_a given by Downing and Williams (1975) and assuming dermis has 65% water content.

§Using value of μ_a given by Vodopyanov (1991) and assuming dermis has 65% water content.

minum electrodes vapor deposited on both sides (AMP Inc., Harrisburg, PA). The construction and characteristics of the transducer have been described previously (Zweig et al., 1993; Venugopalan, 1994). The output voltage $V(t)$ of the transducer generated by a stress transient $\sigma(t)$ is given by (Dyer and Srinivasan, 1986; Schoeffmann et al., 1988)

$$V(t) = \frac{e_{33}}{C_D + C_L} A\sigma(t), \quad (1)$$

where e_{33} is the piezoelectric constant of the PVDF film in pure compression, A is the surface area of the stress affected region, and C_D and C_L are the capacitances of the transducer and the load, respectively. The temporal resolution of the transducer is $\leq$5 ns (Venugopalan, 1994) and provides a consistent response up to a compressive stress of $\sigma = 2 \times 10^{10}$ Pa (Lee et al., 1990). The signal recorded by the digitizer was transferred to a microcomputer (Macintosh LC; Apple Computer, Cupertino, CA) via an RS-232 port.

Fig. 1 is a schematic of the equipment used to obtain the measurements. For experiments employing the TEA CO_2 laser, a 10-mm diameter aperture was used to select a uniform portion of the laser output. The laser beam was propagated through a set of attenuators composed of thin layers of teflon, a 200-mm focal length ZnSe lens, and a gold mirror, which deflected the laser beam onto the surface of the target. The laser pulse energy was constant during the experiment with a pulse-to-pulse variation of $\pm$5% (model J3–09; Molectron Detector, Inc., Portland, OR). The transmission of each attenuator and the ZnSe lens and the reflectance of the mirror were determined beforehand and used to calculate the energy incident on the target surface. The TEA CO_2 laser emitted a multimode beam with an intensity profile uniform to $\pm$20%.

For experiments employing the Q-sw Er:YSGG laser, the laser beam was propagated through a beam splitter, a set of attenuators composed of IR grade quartz, a second beam splitter, and a gold mirror, which deflected the beam 90° through a 95-mm focal length ZnSe lens onto the target surface. The stability of the temporal pulse structure was monitored using a pyroelectric detector (model P5–01; Molectron Detector) with a response time of 500 ps. A second pyroelectric detector (model J3–09; Molectron Detector) measured the energy from the second beam splitter and permitted the energy incident on the target to be determined. The Q-sw Er:YSGG laser emitted a single mode beam with a gaussian intensity profile.

Tissue samples were placed on the transducer surface with a thin layer of saline. The saline provided acoustic contact between the tissue sample and the transducer as well as a source of fluid to avoid dessication of the tissue sample. Samples were sufficiently thick to absorb all delivered radiation. The irradiation resulted in the generation of stresses that traversed the tissue thickness and stressed the piezoelectric film, thereby producing the measured voltages. To ensure that the stress waves remained planar during their transit across the tissue thickness, the laser spots were always greater than 1 mm in diameter. This eliminated geometric attenuation of the stress wave and minimized the effects of acoustic absorption and dispersion on the stress transient using guidelines set forth previously (Sigrist, 1986; Venugopalan, 1994). The large spot size also ensured that the expansion of ablated material away from the target surface took place in a one-dimensional geometry.

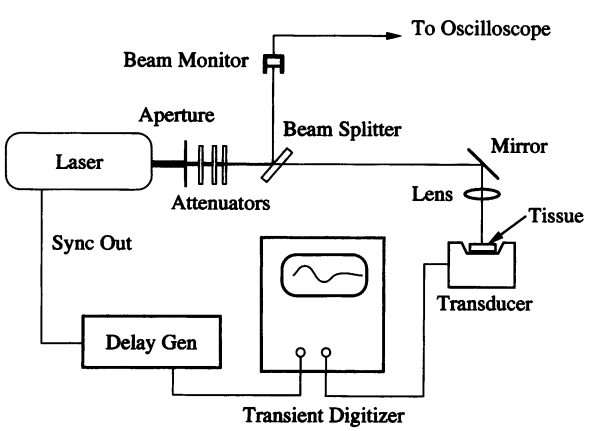

FIGURE 1 Experimental setup for measurement of laser-induced stress transients in tissue.

RESULTS

TEA CO_2 laser experiments

Typical signals from the transducer generated by 10.6-μm (TEA CO_2 laser) irradiation of porcine dermis are shown in Fig. 2. In all figures a positive stress denotes compression. As the stress amplitude varies by three orders of magnitude between the lowest and highest radiant exposures tested, these traces are normalized relative to their peak compressive stress to allow temporal comparison of stress traces generated over this extensive range of radiant exposures. The signals produced by irradiation at radiant exposures ranging from a subablative dose to a strongly ablative dose are represented by traces a–e.

Fig. 2, trace a, is a stress transient generated by a subablative exposure. The stress transient is thermoelastic with the characteristic bipolar signature and reaches its maximum within 55 ns. The stress returns to baseline in approximately 300 ns. When the radiant exposure is equal to the threshold radiant exposure for material removal (Fig. 2, *trace b*), the thermoelastic stress waveform remains unchanged, except for a weak compressive stress, which is observed at late times. When the radiant exposure is increased further (Fig. 2, *trace c*) the magnitude of the second compressive peak rises and cancels a portion of the tensile component of the thermoelastic stress. At larger radiant exposures (Fig. 2, *trace d*), this results in a unipolar stress transient composed of two compressive pulses. The first pulse is generated primarily by the thermoelastic effect and the second by ablative recoil. The rise time of the stress

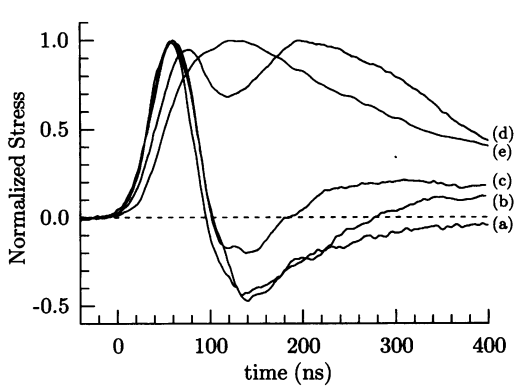

FIGURE 2 Transducer signals resulting from TEA CO_2 laser irradiation of porcine dermis. The radiant exposure and peak compressive stress for each trace are (*a*) $\epsilon_0'' = 4.0 \times 10^3$ J m^{-2}, $\sigma_p = 1.9 \times 10^6$ Pa; (*b*) $\epsilon_0'' = 1.4 \times 10^4$ J m^{-2}, $\sigma_p = 8.0 \times 10^6$ Pa; (*c*) $\epsilon_0'' = 1.9 \times 10^4$ J m^{-2}, $\sigma_p = 1.3 \times 10^7$ Pa; (*d*) $\epsilon_0'' = 3.3 \times 10^4$ J m^{-2}, $\sigma_p = 1.9 \times 10^7$ Pa; (*e*) $\epsilon_0'' = 6.1 \times 10^4$ J m^{-2}, $\sigma_p = 1.5 \times 10^8$ Pa.

transient increases with increasing radiant exposure. At even greater radiant exposures (Fig. 2, *trace e*), the stress transient consists of a single compressive pulse, which reaches a maximum at 130 ns and returns to baseline after 1 μs (not shown) (Dyer and Al-Dhahir, 1990).

The peak compressive stress σ_p is plotted against the incident radiant exposure ϵ_0'' in Fig. 3. For radiant exposures below that required for material removal, the peak stress increases linearly with radiant exposure. However, once the stresses produced by ablative recoil dominate those produced by thermoelastic stress generation, the variation of the peak stress with incident radiant exposure becomes nonlinear.

Q-sw Er:YSGG laser experiments

Typical output signals from the transducer generated by 2.79-μm (Q-sw Er:YSGG laser) irradiation of porcine dermis are shown in Fig. 4. As the stress amplitude varies by three orders of magnitude between the lowest and highest radiant exposures tested, these traces are normalized relative to their peak compressive stress to allow temporal comparison of stress traces generated over this extensive range of exposures. The signals resulting from irradiation of porcine dermis at radiant exposures ranging from a subablative dose to a strongly ablative dose are shown in traces a–d.

Fig. 4, trace a, is a stress transient generated by a subablative exposure. The stress transient is thermoelastic, with a characteristic bipolar signature that reaches its maximum at 45 ns. The stresses return to baseline in approximately 200 ns. When the radiant exposure is raised to a value equal to the threshold radiant exposure for material removal (Fig. 4, *trace b*), the thermoelastic stress waveform remains unchanged at early times, whereas an additional compressive stress is observed at late times. When the radiant exposure is increased further (Fig. 4, *trace c*), the stress transient is unipolar and consists of two compressive pulses. The first pulse is generated primarily through the thermoelastic effect and the second by ablative recoil. The rise time of the stress transient lengthens as the radiant exposure is increased. At the largest radiant exposure (Fig. 4, *trace d*), the stress transient consists of a single unipolar pulse, which reaches its maximum within 80 ns and returns to baseline after 400 ns (not shown).

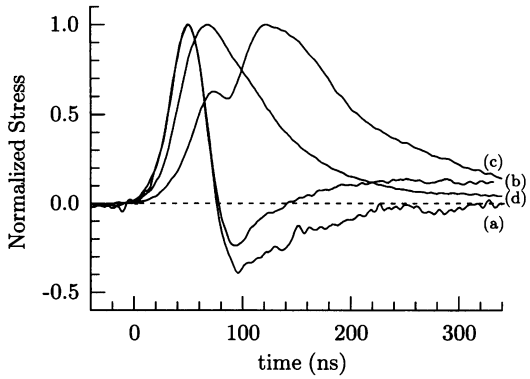

FIGURE 4 Transducer signals resulting from Q-sw Er:YSGG laser irradiation of porcine dermis. The radiant exposure and peak compressive stress for each trace are (*a*) $\epsilon_0'' = 530$ J m^{-2}, $\sigma_p = 1.1 \times 10^5$ Pa; (*b*) $\epsilon_0'' = 1100$ J m^{-2}, $\sigma_p = 2.6 \times 10^5$ Pa; (*c*) $\epsilon_0'' = 1600$ J m^{-2}, $\sigma_p = 2.8 \times 10^5$ Pa; (*d*) $\epsilon_0'' = 2700$ J m^{-2}, $\sigma_p = 4.2 \times 10^6$ Pa.

The peak compressive stress σ_p is plotted against the incident radiant exposure ϵ_0'' in Fig. 5. For radiant exposures below that required for material removal, the peak stress varies linearly with radiant exposure. However, once the stresses produced by ablative recoil dominate those produced by thermoelastic stress generation, the variation of

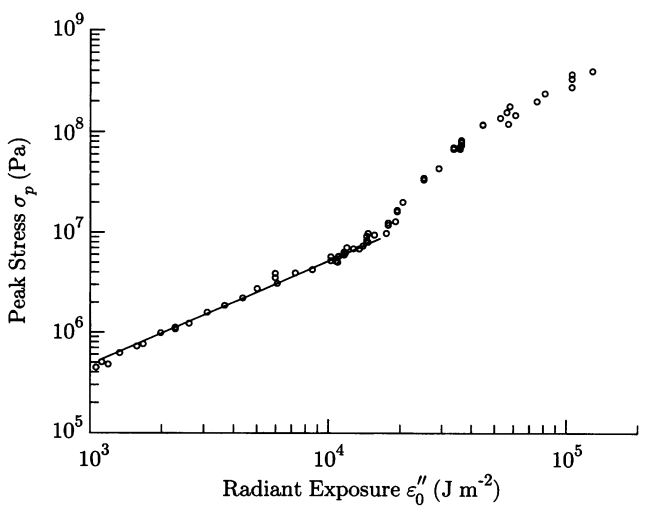

FIGURE 3 Peak compressive stress generated by TEA CO_2 laser irradiation of porcine dermis σ_p versus incident radiant exposure ϵ_0''. The solid line is the best fit of the thermoelastic data to the scaling $\sigma_p \propto \epsilon_0''$.

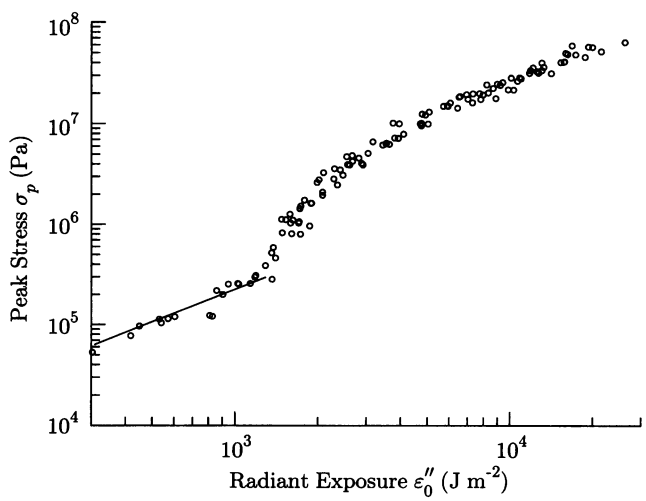

FIGURE 5 Peak compressive stress generated by Q-sw Er:YSGG laser irradiation of porcine dermis σ_p versus incident radiant exposure ϵ_0''. The solid line is the best fit of the thermoelastic data to the scaling $\sigma_p \propto \epsilon_0''$.

the peak stress with incident radiant exposure becomes nonlinear.

ANALYSIS

TEA CO_2 laser irradiation

Two observations regarding the temporal structure of stress transients generated by pulsed TEA CO_2 laser irradiation of porcine dermis require further consideration. First, for radiant exposures where the variation in the peak compressive stress initially becomes nonlinear ($\epsilon_0'' \approx 2 \times 10^4$ J m^{-2}), the stress transient not only has a reduced tensile component when compared to the stress transients generated in the linear regime, but also a second compressive pulse that remains at very long times (>400 ns). This waveform is quite different from those produced by ultraviolet laser irradiation of tissue, where a second compressive pulse is never seen (Venugopalan et al., 1995). As the radiant exposure is increased further, the second compressive pulse increases in magnitude relative to the first and nullifies the tensile component of the thermoelastic stress. This results in a unipolar stress transient with two compressive peaks that merge to form a single compressive stress pulse at higher radiant exposures. The second important observation is that the stress response in the ablative regime occurs on a longer time scale than does the thermoelastic response. This is evidenced by the increase in temporal extent and rise time of the stress transients generated at these radiant exposures. The total duration of the ablative stress transients (~1 μs) (Dyer and Al-Dhahir, 1990) is much longer than those seen in UV laser ablation, where the ablative stress transients return to baseline within 200 ns (Dyer and Al-Dhahir, 1990; Venugopalan et al., 1995). The increases in both the rise time and overall temporal extent of these transients are strong indicators that the majority of material removal occurs after laser irradiation.

When analyzing UV laser ablation of tissue, we previously modeled the material removal process as one of rapid surface vaporization of tissue during irradiation. The model for laser-induced rapid surface vaporization has been presented in detail previously (Venugopalan, 1994; Venugopalan et al., 1995), and only its assumptions and results will be presented here. In this model we assume that surface absorption of the laser irradiance q_0'' creates a high temperature and pressure vapor adjacent to the target surface during irradiation. The expansion velocity of the vapor u_v is assumed to be large compared to the sound velocity in the surrounding medium c_1. This results in the radiation of a shock wave traveling at velocity u_s. Fig. 6 is a schematic of this situation, where the vaporization process is modeled as a piston moving at a velocity u_v into the surrounding gas. Analysis proceeds by solving the mass, momentum, and energy conservation equations across the shock front and results in the following scaling law for the peak recoil stress σ_p:

$$\sigma_p = \Lambda(\epsilon_0'' - \epsilon_{th}'')^{2/3}. \quad (2)$$

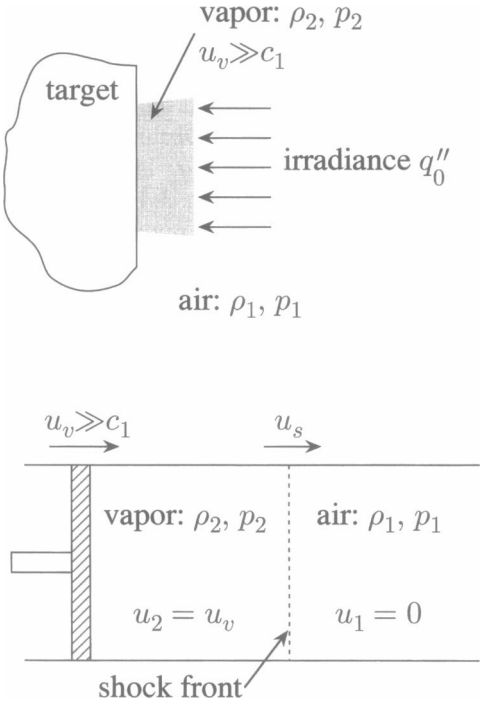

FIGURE 6 Graphic representation of laser ablation of porcine dermis via a process of rapid surface vaporization and a schematic of the piston model used in the process description. Velocities are given in the laboratory reference frame.

Equation 2 is subject to the restriction that Λ does not exceed the value given by the expression

$$\Lambda \le \Lambda_{max} = \left\{\left[\frac{\gamma_1(\gamma_1+1)p_1}{2}\right]^{1/2}\frac{(\gamma_2-1)}{\gamma_2 c_1 t_p}\right\}^{2/3}, \quad (3)$$

where γ_1 and γ_2 are the ratios of specific heats, c_p/c_v, in regions 1 and 2, respectively, and p_1 is the ambient pressure.

For the laser parameters used in this study, $\Lambda_{max} = 5.2 \times 10^4$ kg$^{1/3}$ m^{-1} s$^{-2/3}$ and 4.3×10^4 kg$^{1/3}$ m^{-1} s$^{-2/3}$ for TEA CO_2 and Q-sw Er:YSGG laser ablation, respectively. In Fig. 7 the compressive stress data for TEA CO_2 laser ablation are fit to this scaling law for rapid surface vaporization. Although the agreement between the data and the model prediction is not wholly deficient, the value of the prefactor used to achieve this fit, $\Lambda = 1.68 \times 10^5$ kg$^{1/3}$ m^{-1} s$^{-2/3}$, is more than three times larger than the Λ_{max} allowed for TEA CO_2 laser ablation, thereby violating the constraint imposed by the conservation equations. Thus rapid surface vaporization appears to be inconsistent with the measured stresses because the ablated material leaves the tissue surface with a kinetic energy greater than that allowed by this process.

Given that the magnitude of the ablative recoil stresses is greater than that allowed by rapid surface vaporization and the temporal structure of the stress transients indicates that the majority of the material removal occurs after irradiation, we consider material removal to occur explosively, using a model initially formulated by Phipps and co-workers (Phipps et al., 1990), as shown schematically in Fig. 8. In

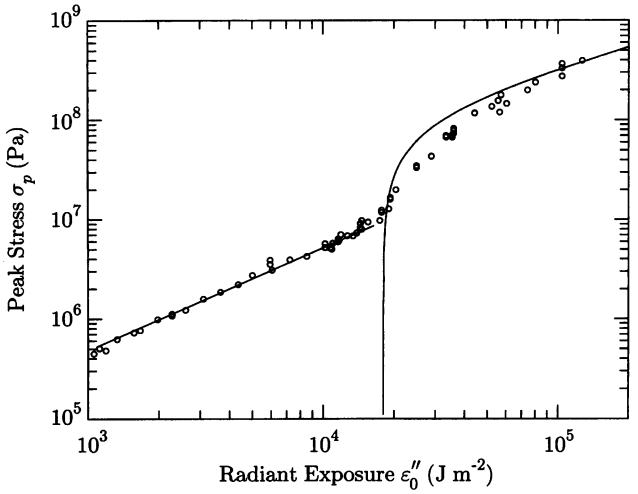

FIGURE 7 Peak compressive stress generated by TEA CO_2 laser irradiation of porcine dermis σ_p versus incident radiant exposure ϵ_0''. The line is the best fit of the thermoelastic data to the scaling $\sigma_p \propto \epsilon_0''$. The curve is the best fit of the ablative recoil data to the scaling law for rapid surface vaporization given by $\sigma_p = \Lambda(\epsilon_0'' - \epsilon_{th}'')^{2/3}$, where $\Lambda = 1.68 \times 10^5$ kg$^{1/3}$ m^{-1} s$^{-2/3}$ and $\epsilon_{th}'' = 1.8 \times 10^4$ J m^{-2}.

this case, we assume that the entire laser pulse energy is absorbed according to Beer's law before the onset of material removal. If the energy deposition occurs on a time scale where losses are negligible, the spatial profile of the volumetric energy density $\epsilon'''(x)$ within the target at the end of the laser pulse is given by

$$\epsilon'''(x) = \mu_a \epsilon_0'' \exp(-\mu_a x). \tag{4}$$

Assuming that a threshold energy density $\mu_a \epsilon_{th}''$ is required to affect material removal, the mass removed per unit area m'' is given by

$$m'' = \frac{\rho}{\mu_a} \ln\left(\frac{\epsilon_0''}{\epsilon_{th}''}\right) = \frac{\rho}{\mu_a} \ln \eta, \tag{5}$$

where ρ is the tissue mass density and η is the ratio between the incident and threshold radiant exposures. For $0 \leq x < \delta_{etch}$, with $\delta_{etch} = m''/\rho$, the delivered energy density exceeds that necessary for material removal. If we scale this excess energy, ϵ_{excess}'', with the kinetic energy imparted to the ablated mass, we have

$$\epsilon_{excess}'' = \int_0^{\delta_{etch}} \mu_a[\epsilon_0'' \exp(\mu_a x) - \epsilon_{th}''] dx \propto \frac{l''^2}{2m''}. \tag{6}$$

The linear momentum per unit area of the ablated material l'' is the time integral of the recoil stress at the target surface and should scale with the product of the peak stress σ_p and the laser pulse duration. Thus we have

$$l'' = \int_0^{\infty} \sigma(t) dt \propto \sigma_p t_p. \tag{7}$$

We eliminate m'' and l'' by substituting Eqs. 5 and 7 into Eq. 6. Solving for σ_p yields the following scaling law for the peak compressive recoil stresses generated by an explosive material removal process:

$$\sigma_p = \Upsilon\left[\frac{2\rho\epsilon_0''}{\mu_a t_p^2} \ln \eta\left(1 - \frac{1}{\eta} - \frac{\ln \eta}{\eta}\right)\right]^{1/2}. \tag{8}$$

This scaling law has two adjustable parameters, the threshold radiant exposure for material removal ϵ_{th}'' and the dimensionless multiplicative constant Υ. However, the value of ϵ_{th}'' is constrained, as it must be consistent with the radiant exposure at which a transition from a thermoelastic to an ablative response is observed in the temporal structure of the measured stress transients. Fig. 9 is a plot of the stresses generated by ablative recoil and the best fit to the scaling law given by Eq. 8 with $\Upsilon = 0.124$ and $\epsilon_{th}'' = 1.3 \times 10^4$ J m^{-2}. Equation 8 provides a better fit to the data than the scaling law for rapid surface vaporization. Note that the

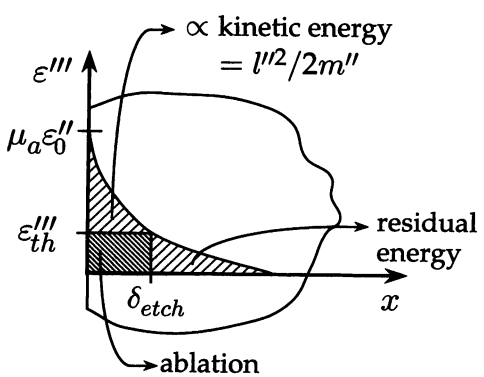

FIGURE 8 Schematic of the model used to describe explosive material removal. See text for details.

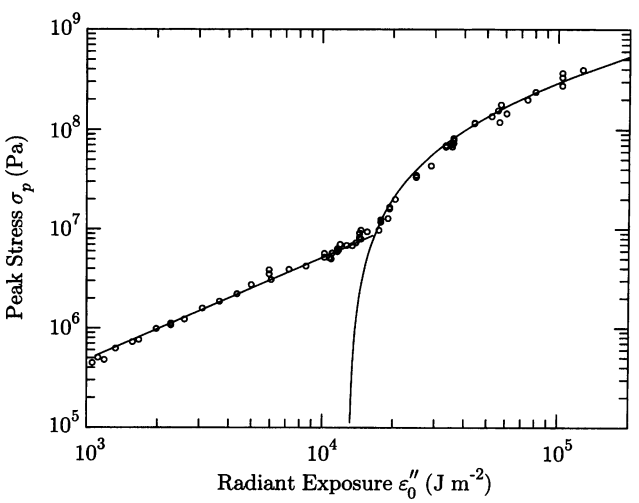

FIGURE 9 Peak compressive stress generated by TEA CO_2 laser irradiation and ablation of porcine dermis σ_p versus incident radiant exposure ϵ_0''. The curve is the best fit of the ablative recoil data to the scaling law for explosive material removal. The parameters of the curve fit are $\Upsilon = 0.124$ and $\epsilon_{th}'' = 1.3 \times 10^4$ J m^{-2}.

value of ϵ''_{th} given by the experimental results is approximately a factor of 2 smaller than most values reported in the literature (Walsh and Deutsch, 1988; Green et al., 1990). However, it is likely that the measurement of the recoil stresses generated by material removal is a more accurate means of determining the threshold radiant exposure for ablation than extrapolations from gross material removal data.

Q-sw Er:YSGG laser irradiation

The stress transients generated by Er:YSGG laser irradiation are similar in many respects to those produced by TEA CO_2 laser irradiation. When attempting to fit the ablative recoil data of Q-sw Er:YSGG laser ablation we find, as in the case of TEA CO_2 laser irradiation, that the model for rapid surface vaporization fails to provide an adequate scaling law for the measurements. This is not surprising, because studies of the plume dynamics for Q-sw erbium laser ablation of tissue have revealed the process to be explosive and to occur with a time delay with respect to irradiation (Walsh and Deutsch, 1991). This being the case, we fit the Q-sw Er:YSGG ablative recoil data to the scaling law for explosive material removal as developed above. The result of this is shown in Fig. 10, with $\Upsilon = 0.124$ and $\epsilon''_{th} = 1200$ J m^{-2}. As in the case for TEA CO_2 laser ablation, the value for ϵ''_{th} is smaller than values reported in the literature (Ren et al., 1992). Interestingly, the value for the dimensionless scaling factor Υ is identical for both TEA CO_2 and Q-sw Er:YSGG ablation events and indicates that the same fraction of "excess energy" is partitioned to the kinetic energy of the ablated products.

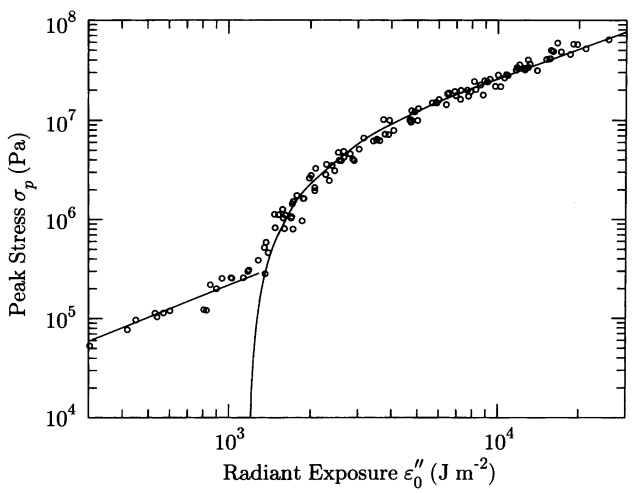

FIGURE 10 Peak compressive stress generated by Q-sw Er:YSGG laser irradiation and ablation of porcine dermis σ_p versus incident radiant exposure ϵ''_0. The curve is the best fit of the ablative recoil data to the scaling law for explosive material removal. The parameters of the curve fit are $\Upsilon = 0.124$ and $\epsilon''_{th} = 1200$ J m^{-2}.

DISCUSSION

The results of this study demonstrate that the stress transients resulting from TEA CO_2 and Q-sw Er:YSGG laser ablation of porcine dermis can be accurately modeled as a process of explosive material removal. The entire laser pulse energy is delivered before significant material removal occurs and the tissue volume that reaches a threshold volumetric energy density (ϵ'''_{th}) is explosively removed. Furthermore, the kinetic energy of the ablated material scales with the amount of energy in excess of ϵ'''_{th} delivered to the tissue volume removed.

Both TEA CO_2 and Q-sw Er:YSGG laser ablation proceed explosively, despite the fact that mechanical equilibration of the heated layer is allowed (i.e., $\tau_m > \mathcal{O}(1)$) only for Q-sw Er:YSGG irradiation. The photomechanical basis of ablation proposed by Albagli and co-workers (Albagli et al., 1994b) predicts that when stresses generated within tissue have sufficient time to equilibrate, the contribution of photothermal mechanisms to the ablation process increase, and thermal decomposition rather than an explosive or photomechanical process of material removal occurs. In addition, the authors maintain that the threshold energy density for the onset of material removal should increase once mechanical equilibration is achieved, because ablation via vaporization alone requires more energy per unit volume than material fracture.

These propositions appear inconsistent with the experimental findings. Using values of μ_a cited in Table 1 and keeping in mind that for a gaussian beam (used in the Er:YSGG laser experiments) the radiant exposure at the center of the laser beam is twice the average incident radiant exposure ϵ''_0, the maximum energy per unit mass deposited into the tissue water at ablation threshold is 7.2×10^5 and 8.0×10^5 J kg^{-1}, respectively, for TEA CO_2 and Q-sw Er:YSGG laser ablation of tissue. That is, ϵ'''_{th} is roughly comparable between the two wavelengths, even though τ_m is nearly an order of magnitude larger for Q-sw Er:YSGG laser irradiation relative to TEA CO_2 laser irradiation (cf. Table 1). In addition, the energy per unit mass delivered to the tissue at the ablation threshold is in both cases larger than the sensible heat of water under STP conditions (3.28×10^5 J kg^{-1}) but significantly smaller than the sum of the sensible and latent heats of vaporization under STP conditions (2.58×10^6 J kg^{-1}). This demonstrates that complete vaporization of the heated volume is not achieved at ablation threshold and implicates a significant photomechanical component in the material removal process.

The inconsistencies between the experimental findings and current photomechanical models for tissue ablation probably stem from simplifications made within the model formulation. The general concept that smaller optical absorption coefficients and laser pulse durations reduce mechanical equilibration of a heated volume during irradiation and result in a photomechanical material removal process is likely to be correct. However, this concept is based on two assumptions that are not met in

many tissue ablation processes. First, it is explicitly assumed that the absorbed laser radiation is distributed evenly within the local tissue volume (Albagli et al., 1994b). This assumption is valid only when $\mathrm{Fo}_\delta \geq \mathcal{O}(1)$, which depends on the tissue morphology and optical properties as well as the laser pulse duration. Second, one implicitly assumes that when inertial confinement is not achieved during irradiation, the tissue has access to a pathway for thermal decomposition. However, if the tissue structural matrix receives a negligible amount of energy via optical absorption and transport (diffusive and radiative), this assumption is not satisfied. Thus in this case, the mechanical integrity of the structural matrix is not compromised, and it can deform with the expansion of the heated water until it fractures under the stresses generated.

In summary, the use of a measure for inertial confinement or mechanical equilibration (e.g., τ_m) as an indicator for a photothermal versus photomechanical mechanism of material removal is valid only when the tissue structural matrix has access to a pathway for thermal decomposition and the kinetics of the decomposition process are much faster than the time scale of irradiation. However, when the chromophore is a tissue constituent other than the structural matrix under conditions where either energy transport and/or thermal decomposition is not operative, a measure of inertial confinement is no longer a valid indicator for the mechanism of material removal. If the characteristic time scale for matrix decomposition is shorter than the irradiation time, as is likely for collagenous tissues (Venugopalan et al., 1995), energy transport from the heated tissue constituents to the tissue structural matrix (i.e., $\mathrm{Fo}_\delta \geq \mathcal{O}(1)$) is a necessary condition to achieve a transition from a photomechanical to a photothermal mode of material removal.

Despite the fact that $\mathrm{Fo}_\delta \geq \mathcal{O}(1)$ seems to be a valid parameter to indicate the transition from an explosive to a surface-mediated material removal process, it is a condition that is necessary but not sufficient. If it were a sufficient condition, all ablation processes that target a material unable to withstand stresses (e.g., a liquid) and allow for mechanical equilibration during irradiation would result in a removal process characterized by surface vaporization without any explosive component. However, several experimental studies have demonstrated that this is not the case. For example, when nanosecond laser pulses are employed to convert liquid water to vapor, the transition exhibits a decidedly explosive characteristic (Askar'yan et al., 1963; Emmony et al., 1976; Venugopalan et al., manuscript in preparation). This characteristic of the phase transition is likely due to the high volumetric power densities achieved by the laser irradiation such that the rate of energy consumption by vaporization from the surface and nucleation of bubbles below the surface are insufficient to prevent the tissue water from being superheated to the spinodal limit. When this superheat limit is reached, the liquid water is mechanically unstable and a rapid phase transition to vapor is forced by a process known as spinodal decomposition or flash boiling (Eberhart and Schnyders, 1973; Skripov, 1974). At atmospheric pressure the maximum superheat temperature of water is theoretically estimated to be 305°C, whereas 280°C is the highest superheat temperature achieved to date.

The process of flash boiling has been proposed as the mechanism for pulsed ablation of tissue as well (Esenaliev et al., 1989; Oraevsky et al., 1992). This mechanism becomes even more plausible when one considers that in tissue the nucleation and growth of subsurface vapor bubbles are strongly suppressed because of the stiffness of the surrounding structural matrix, which results in significant superheating of the surrounding tissue water. However, no analysis has yet been presented to firmly establish the conditions under which this process is operative. To superheat water within the tissue bulk to the spinodal limit, the rate of energy deposition must be much larger than the rate of energy consumption by the growth of bubble nucleation centers within the tissue, i.e.,

$$q'''_{sp} \gg \rho_v h_{fg} \Omega V(t_p), \tag{9}$$

where q'''_{sp} is the volumetric power density necessary to achieve spinodal conditions, ρ_v is the density of the vapor inside the bubbles, h_{fg} is the latent heat of vaporization, Ω is the number density of nucleation sites, and $V(t_p)$ is the volume of each nucleation site at the end of the laser pulse, $t = t_p$. To evaluate this expression we must estimate both the volume of vapor contained within these sites at the end of the laser pulse $V(t = t_p)$ and the number density of nucleation sites Ω.

To estimate the volume of a single nucleation site at the end of the laser pulse we must calculate the bubble growth over time. It is known that in a liquid pool the growth of a bubble, in its early stages, is limited by the energy necessary to displace the liquid surrounding it (inertia-controlled growth), whereas at a later stage the growth becomes limited instead by the energy required to form the necessary vapor (heat transfer controlled growth). Note that an analysis based on either of these two cases represents an upper bound for both $V(t)$ and q'''_{sp}, because factors that limit the rate of bubble growth, such as the energy necessary to strain the surrounding structural matrix of the tissue, are ignored. The bubble radius $R(t)$ in the inertia-controlled regime is given by (Rayleigh, 1917; Mikić et al., 1970)

$$R(t) = \left[\frac{2(p_v - p_\infty)}{3\rho_f}\right]^{1/2} t, \tag{10}$$

whereas in the heat transfer controlled regime $R(t)$ is given by (Plesset and Zwick, 1954; Mikić et al., 1970)

$$R(t) = \left[\frac{\rho_f c_f (T_\infty - T_{sat})}{\rho_v h_{fg},}\right]\left(\frac{12\alpha_f}{\pi} t\right)^{1/2}. \tag{11}$$

In these expressions, p_∞ and T_∞ are the pressure and temperature of the surrounding superheated liquid; T_{sat} is the saturation temperature corresponding to the pressure p_∞; p_v

and ρ_v are the pressure and density of vapor within the bubble and ρ_f, c_f, and α_f are the density, specific heat, and thermal diffusivity of the surrounding liquid. In the inertia-controlled case, the vapor pressure within the bubble is taken as the saturation pressure of vapor at the maximum superheat temperature of the surrounding liquid (i.e., 305°C) and gives an upper bound for the bubble radius. Similarly, for the heat transfer controlled case the temperature of the vapor within the bubble is taken as the saturation temperature at the pressure of the surrounding liquid. This maximizes the temperature difference across the bubble interface and again maximizes the bubble radius.

For the inertia-controlled case, it is more convenient to express the vapor bubble growth in terms of temperature rather than pressure. For water, the saturation pressure is related to the saturation temperature through the empirical expression $p_{sat} = a \exp(-b/T_{sat})$, where $a = 3.0705 \times 10^{10}$ Pa and $b = 4688.2$ K (Weast, 1985). Substituting this expression into Eq. 10 and integrating gives the following expression for $V(t)$ in the inertia-controlled bubble growth case:

$$V(t) = \frac{4\pi}{3}\left\{\frac{2a}{3\rho_f}[\exp(-b/T_v) - \exp(-b/T_{sat})]\right\}^{3/2} t^3, \quad (12)$$

whereas for the heat transfer mediated case we have

$$V(t) = \frac{4\pi}{3}\left[\frac{\rho_f c_f (T_\infty - T_{sat})}{\rho_v h_{fg},}\right]^3 \left(\frac{12\alpha_f}{\pi} t\right)^{3/2}. \quad (13)$$

Substituting Eq. 12 into Eq. 9 gives the expression for the incident volumetric power density necessary to achieve flash boiling when the bubble growth is controlled by the inertia of the surrounding liquid:

$$q_0''' \gg q_{sp}''' = \frac{4\pi\rho_v h_{fg}\Omega t_p^2}{3} \times \left\{\frac{2a}{3\rho_f}[\exp(-b/T_v) - \exp(-b/T_{sat})]\right\}^{3/2}. \quad (14)$$

Alternatively, substituting Eq. 13 into Eq. 9 gives the expression for the incident volumetric power density necessary to achieve flash boiling when the bubble growth is controlled by heat transfer considerations:

$$q_0''' \gg q_{sp}''' = \frac{4\pi\rho_v h_{fg}\Omega t_p^{1/2}}{3} \times \left[\frac{\rho_f c_f (T_\infty - T_{sat})}{\rho_v h_{fg},}\right]^3 \left(\frac{12\alpha_f}{\pi}\right)^{3/2}. \quad (15)$$

The only unknown on the right-hand side of the above equations is the density of nucleation centers Ω. To produce an order of magnitude estimate for the density of nucleation centers present within tissue, we proceed as follows. Because the results thus far indicate that no significant material removal occurs during irradiation, the maximum volume that the vapor bubbles can occupy immediately at the end of irradiation is on the order of the heated volume, and thus $\Omega V(t_p) \approx 1$. Because bubble growth that occurs over a characteristic duration of $t_p \approx 100$ ns is in the inertia-controlled regime (as will be demonstrated shortly), we substitute the spinodal and saturation temperatures of water at atmospheric pressure, $T_v = 305$°C and $T_{sat} = 100$°C, into Eq. 12 to give $V(t = 100\ \text{ns}) = 10^{-15}$ m^3, which yields $\Omega = 10^{15}$ m^{-3}.

We can now obtain a numerical estimate for the volumetric power density necessary to achieve flash boiling. Using the values for T_v and T_{sat} stated above in Eqs. 14 and 15, we plot q_{sp}''' versus laser pulse duration t_p with Ω as a parameter in Fig. 11. Note that for exposures less than ~3 μs, the bubble growth is mediated by the inertia of the surrounding liquid, whereas for longer exposures the bubble growth is limited by heat transfer from the superheated liquid into the vapor. Values of the incident volumetric power density achieved by our experiments at ablation threshold q_{th}''' are shown, as well as values for q_{th}''' typically achieved for 100 μs CO_2 and Er:YAG laser exposures (Frenz et al., 1989). This figure clearly indicates that the incident volumetric power density is sufficient to drive the tissue liquid to the spinodal limit and result in explosive boiling for nanosecond laser exposures.

This analysis is also consistent with the results of studies examining the dynamics of CO_2 and Er:YAG/YSGG laser ablation of tissue using pulses on the order of 100 μs in duration. Such studies have established that tissue ablation at these wavelengths and pulse durations result in material removal during irradiation, not via explosion but through a surface-mediated process of thermal liquefaction followed by molten tissue ejection and vaporization (Zweig and We-

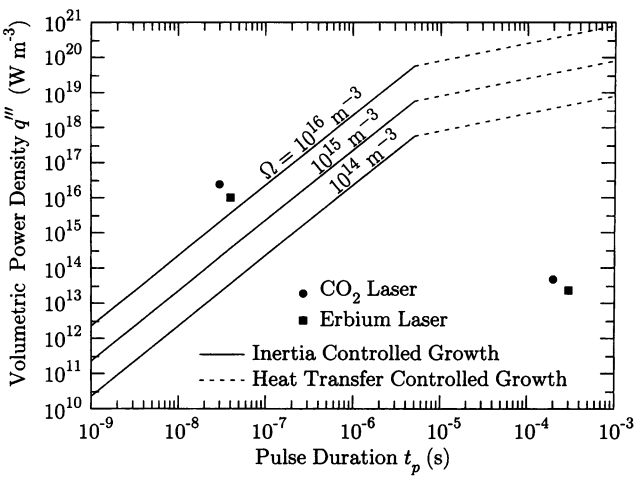

FIGURE 11 The solid and dotted lines represent the volumetric power density q_{sp}''' necessary to achieve flash boiling of tissue water versus laser pulse duration t_p with the number density of nucleation sites Ω as a free parameter. The data points represent the volumetric power density achieved at the ablation threshold q_{th}''' for different pulse durations. See text for further details.

ber, 1987; Zweig, 1991a; Zweig, 1991b). This is consistent with our theoretical framework, because although tissue water continues to be the dominant chromophore in these cases, thermal diffusion during the longer laser pulse does not provide microscale thermal confinement, as Fo_δ is usually between 3 and 30 in these cases and the volumetric power densities at the ablation threshold at these longer pulse durations are not in excess of q'''_{sp}, as shown by Fig. 11.

Finally, we must check that the radiant exposure at the ablation threshold is sufficient to heat the tissue water to the spinodal limit. The change in temperature at the tissue surface is given by

$$\Delta T = \frac{\mu_a \epsilon''_0}{\rho_{H_2O} c_{v,H_2O} x_{H_2O}}. \quad (16)$$

Using this equation we find that the temperature change achieved at the ablation threshold is 260°C for TEA CO_2 laser irradiation, but only 147°C for Q-sw Er:YSGG laser irradiation. However, the beam profile of the Q-sw Er:YSGG laser used was gaussian, and thus the radiant exposure at the center of the beam is double the value computed using pulse energy divided by the $1/e^2$ spot size. Taking this into account, the maximum temperature change at the tissue surface is 290°C for Er:YSGG irradiation. Both values for ΔT are sufficient to heat the tissue water to the spinodal limit from an initial room temperature of 22°C, and their values are consistent with the minimum ΔT required, 258–293°C.

With this analysis, it is instructive to contrast the ablation mechanism of short-pulse IR laser ablation with UV laser ablation, where material removal proceeds through rapid surface vaporization during irradiation. Although the mechanism for material removal is fundamentally different between IR and UV ablation, the values of τ_m, Fo, and Fo_δ characterizing the laser-tissue interaction are nearly identical for KrF-excimer and TEA CO_2 laser irradiation and for ArF-excimer and Q-sw Er:YSGG laser irradiation, respectively (Venugopalan et al., 1995). Consideration of the tissue chromophore, microscale thermal confinement, and available decomposition pathways are all important to understanding the differences in thermal and mechanical injury produced by UV and IR laser ablation. For UV ablation, material removal is achieved through targeted destruction of the tissue chromophore (collagen) and implies that all of the denatured collagen is removed. This may be the reason why the morphology of in vitro ArF- and KrF-excimer laser ablation of tissue is free of gross mechanical injury and exhibits minimal thermal injury (Lane et al., 1985; Puliafito et al., 1985; Puliafito et al., 1987). By contrast, ablation using IR sources such as Q-sw Er:YAG and TEA CO_2 lasers leaves the matrix relatively intact because of microscale thermal confinement, and the large volumetric power densities achieved by the tissue heating result in an explosive ablation process with increased recoil stresses. These recoil stresses can result in gross mechanical tearing at the margins of the incision (Cummings and Walsh, 1993b). In addition, as the mechanism and dynamics of IR ablation do not ensure the removal of all the heated liquid, the thermal injury resulting from this tends to be more extensive than from UV ablation (Walsh et al., 1988; Walsh et al., 1989), despite comparable optical absorption depths.

Although the process of explosive material removal is fully consistent with the detailed mechanism of spinodal decomposition or flash boiling of the heated tissue water, other mechanisms remain viable options for explaining the material removal process. For example, Albagli and coworkers have observed that subthreshold irradiation of soft tissues under inertially confined conditions results in surface deformations consistent with the nucleation of subsurface vapor bubbles formed by the propagation of the tensile component of the thermoelastic wave (Albagli et al., 1994a). At higher radiant exposures, it is thought that the dynamics of these bubbles may induce tissue disruption mediated by cavitation. While this may be the mechanism for TEA CO_2 laser ablation, it is unlikely to be the mechanism for Q-sw Er:YSGG laser ablation. This is because the negative component of the thermoelastic stress transient has a magnitude of only $\sim 3 \times 10^5$ Pa, which is insufficient to induce cavitation in free water or under conditions where the water is confined within a structural tissue matrix (Fisher, 1948). Other processes that may provide valid descriptions of the events leading to material removal in pulsed IR laser ablation where microscale thermal confinement is achieved include the following:

1. Tensile stresses generated by the thermoelastic mechanism promote the nucleation of subsurface vapor bubbles, and the subsequent growth dynamics of the bubbles disrupt the tissue structural matrix, leading to fracture and explosive removal (TEA CO_2 ablation only).
2. Laser irradiation results in heating and vaporization of water at the tissue surface, and once this small amount of water is removed, the water below the tissue surface is heated and vaporized but cannot escape, because the structure remains intact and restrains the expansion of the heated liquid and vapor. This leads to an increase in temperature and pressure below the tissue surface that results in tissue fracture and explosive removal.
3. The sequence of events is identical to that in 2, with the exception that the onset of material removal is triggered not by stresses that exceed the ultimate tensile strength of the native tissue but by denaturation of the collagen, which causes an abrupt reduction in the ultimate tensile strength of the tissue and results in sudden fracture and explosive removal of tissue.

The first option is only viable for TEA CO_2 ablation for the reasons noted above. The second has been proposed by other investigators (Verdaasdonk et al., 1990; LeCarpentier et al., 1993), albeit within the context of continuous-wave laser ablation. The third option is pos-

sible because the energy density achieved in the collagen fibrils is approximately one-quarter of that in the free tissue water, so that tissue collagen may be denatured before the onset of material removal. As such the abrupt loss of tissue strength that occurs with this process may be the event that triggers the explosion. The difference between the situations described in 1 and 2 is important. The first refers to a process of cavitation where the vapor density within the bubbles is small. As such the dynamics of the bubbles, and thus tissue fragmentation, is governed solely by the inertia and mechanical properties of the surrounding tissue. However, in the second case, the vapor density is much larger and latent heat flow may also be a factor that affects the bubble growth dynamics and tissue fracture (Plesset and Prosperetti, 1977). It should also be noted that situation 2 may be further complicated by the possibility that the compressive recoil associated with surface evaporation occurring during irradiation may suppress bubble nucleation. Thus the cessation of this evaporation, which occurs at the end of irradiation, will lead to a pressure drop within the heated volume and may be the event that triggers the subsurface bubble growth and subsequent explosive removal of tissue. Only further experimental study will conclusively resolve the viability of each of these mechanisms and the conditions under which they are operative.

CONCLUSIONS

The stress transients generated by pulsed laser irradiation and ablation of porcine dermis at $\lambda = 2.79$ μm and 10.6 μm have been measured. Laser exposures that do not achieve material removal produce stress transients consistent with thermoelastic stress generation. When ablation is achieved, the recoil stresses produced at both wavelengths suggest that the bulk of material removal occurs with a delay relative to irradiation and proceeds via tissue fracture and explosive material removal. This permits the formulation of a scaling law, which relates the measured recoil stress with the incident and threshold radiant exposures.

The results suggest that when water is the dominant chromophore, and microscale thermal confinement is achieved during nanosecond laser irradiation, the material removal process is explosive. This occurs because the tissue does not have access to a pathway for thermal decomposition and the characteristic pathway for the phase transition of water under these conditions is through flash boiling. The experimental results also support the hypothesis that this photomechanical mode of material removal is insensitive to the achievement of mechanical equilibration during irradiation. Instead, when the kinetics of the thermal decomposition process is faster than the primary mode of energy transport within the tissue, the transition from a photomechanical to a photothermal mode for material removal is given by a microscale Fourier number, $Fo_\delta \equiv \alpha t_p/\delta^2$. Once sufficient time is available during the laser irradiation for the deposited laser energy to diffuse into the tissue structural matrix, the thermal pathway for decomposition becomes accessible and a transition from a photomechanical to a photothermal mode of material removal is achieved. This is seen experimentally when comparing nanosecond with microsecond pulsed IR laser ablation. Specifically, the inability of microsecond-long IR laser pulses to deliver large volumetric power densities as well as achieve microscale thermal confinement results in a material removal process that follows a purely photothermal rather than photomechanical pathway.

The explosive ablation mechanism operative for infrared laser ablation where microscale thermal confinement is achieved may account for the differences in tissue morphology between pulsed UV and IR laser ablation. Because tissue collagen is the primary chromophore for UV laser ablation, tissue that is decomposed is removed. However, the inability of IR wavelengths, whose dominant tissue chromophore is water, to directly decompose the tissue structure leads to an explosive removal process, resulting in significant thermal and gross mechanical injury to the remaining tissue.

We thank Barry Payne and Andrew Yablon for their critical review of the manuscript and assistance with the erbium laser experiments.

We acknowledge the support of the Whitaker Foundation through a Biomedical Engineering Research Grant. Portions of this work were supported by the U.S. Army Medical Research and Development Command under contract DAMD-17-94-C-4009. The views, opinions, and/or findings contained in this report are those of the authors and should not be construed as an official Department of the Army position, policy, or decision.

REFERENCES

Albagli, D., B. Banish, M. Dark, G. S. Janes, C. von Rosenberg, L. Perelman, I. Itzkan, and M. S. Feld. 1994a. Interferometric surface monitoring of biological tissue to study inertially confined ablation. *Lasers Surg. Med.* 14:374–385.

Albagli, D., L. T. Perelman, G. S. Janes, C. von Rosenberg, I. Itzkan, and M. S. Feld. 1994b. Inertially confined ablation of biological tissue. *Lasers Life Sci.* 6:55–68.

Anderson, R. R., and J. A. Parrish. 1983. Selective photothermolysis: precise microsurgery by selective absorption of pulsed radiation. *Science.* 220:524–527.

Askar'yan, G. A., A. M. Prokhorov, G. F. Chanturiya, and G. P. Shipulo 1963. The effects of a laser beam in a liquid. *Sov. Phys. JETP.* 17: 1463–1465.

Cummings, J. P., and J. T. Walsh, Jr. 1993a. Erbium laser ablation: the effect of dynamic optical properties. *Appl. Phys. Lett.* 62:1988–1990.

Cummings, J. P., and J. T. Walsh, Jr. 1993b. Tissue tearing caused by pulsed laser-induced ablation pressure. *Appl. Opt.* 32:494–503.

Downing, H. D., and D. Williams. 1975. Optical constants of water in the infrared. *J. Geophys. Res.* 80:1656–1661.

Dyer, P. E., and R. K. Al-Dhahir. 1990. Transient photoacoustic studies of laser tissue ablation. *Proc. SPIE.* 1202:46–60.

Dyer, P. E., and R. Srinivasan. 1986. Nanosecond photoacoustic studies on ultraviolet laser ablation of organic polymers. *Appl. Phys. Lett.* 48: 445–447.

Eberhart, J. G., and H. C. Schnyders. 1973. Application of the mechanical stability condition to the prediction of the limit of superheat for normal alkanes, ether, and water. *J. Phys. Chem.* 77:2730–2736.

Ediger, M. N., G. H. Pettit, and D. W. Hahn. 1994. Enhanced ArF laser absorption in a collagen target under ablative conditions. *Lasers Surg. Med.* 15:107–111.

Ediger, M. N., G. H. Pettit, R. P. Weiblinger, and C. H. Chen. 1993. Transmission of corneal collagen during ArF excimer laser ablation. *Lasers Surg. Med.* 13:204–210.

Edwards, G., R. Logan, M. Copeland, L. Reinisch, J. Davidson, B. Johnson, R. Maciunas, M. Mendenhall, R. Ossoff, J. Tribble, J. Werkhaven, and D. O'Day. 1994. Tissue ablation by a free-electron laser tuned to the amide II band. *Nature.* 371:416–419.

Emmony, D. C., B. M. Geerken, and A. Straaijer. 1976. The interaction of 10.6 μm laser radiation with liquids. *Infrared Phys.* 16:87–92.

Esenaliev, R. O., A. A. Oraevsky, and V. S. Letokhov. 1989. Laser ablation of atherosclerotic blood vessel tissue under various irradiation conditions. *IEEE Trans. Biomed. Eng.* 36:1188–1194.

Fisher, J. C. 1948. The fracture of liquids. *J. Appl. Phys.* 19:1062–1067.

Frenz, M., V. Romano, A. D. Zweig, H. P. Weber, N. I. Chapliev, and A. V. Silenok. 1989. Instabilities of laser cutting of soft media. *J. Appl. Phys.* 66:4496–4503.

Green, H. A., Y. Domankevitz, and N. S. Nishioka. 1990. Pulsed carbon dioxide laser ablation of burned skin: in vitro and in vivo analysis. *Lasers Surg. Med.* 10:476–484.

Hahn, D. W., M. N. Ediger, and G. H. Pettit. 1995. Dynamics of ablation plume particles generated during excimer laser corneal ablation. *Lasers Surg. Med.* 16:384–389.

Kitai, M. S., V. L. Popkov, V. A. Semchishen, and A. A. Kharizov. 1991. The physics of UV laser cornea ablation. *IEEE J. Quantum Elec.* 27:302–307.

Lane, R. J., R. Linsker, J. J. Wynne, A. Torres, and R. G. Geronemus. 1985. Ultraviolet-laser ablation of skin. *Arch. Dermatol.* 121:609–617.

Lane, R. J., J. J. Wynne, and R. G. Geronemus. 1987. Ultraviolet laser ablation of skin: healing studies and a thermal model. *Lasers Surg. Med.* 6:504–513.

LeCarpentier, G. L., M. Motamedi, L. P. McMath, S. Rastegar, and A. J. Welch. 1993. Continuous wave laser ablation of tissue: analysis of thermal and mechanical events. *IEEE Trans. Biomed. Eng.* 40:188–200.

Lee, L. M., D. A. Hyndman, R. P. Reed, and F. Bauer. 1990. PVDF applications in shock measurements. *In* Shock Waves in Condensed Matter—1989. S. C. Schmidt, J. N. Johnson, and L. W. Davison, editors. Elsevier Science Publishers, Amsterdam. 821–824.

Mikić, B. B., W. M. Rohsenow, and P. Griffith. 1970. On bubble growth rates. *Int. J. Heat Mass Transfer.* 13:657–666.

Oraevsky, A. A., R. O. Esenaliev, and V. S. Letokhov. 1992. Temporal characteristics and mechanism of atherosclerotic tissue ablation by nanosecond and picosecond laser pulses. *Lasers Life Sci.* 5:75–93.

Phipps, C. R., Jr., R. F. Harrison, T. Shimada, G. W. York, T. P. Turner, X. F. Corlis, H. S. Steele, L. C. Haynes, and T. R. King. 1990. Enhanced vacuum laser-impulse coupling by volume absorption at infrared wavelengths. *Lasers Particle Beams.* 8:281–297.

Plesset, M. S., and A. Prosperetti. 1977. Bubble dynamics and cavitation. *Annu. Rev. Fluid. Mech.* 9:145–185.

Plesset, M. S., and S. A. Zwick. 1954. The growth of vapor bubbles in superheated liquids. *J. Appl. Phys.* 25:493–500.

Puliafito, C. A., R. F. Steinert, T. F. Deutsch, F. Hillenkamp, E. J. Dehm, and C. M. Adler. 1985. Excimer laser ablation of the cornea and lens. *Ophthalmology.* 92:741–748.

Puliafito, C. A., K. Wong, and R. F. Steinert. 1987. Quantitative and ultrastructural studies of excimer laser ablation of the cornea at 193 and 248 nanometers. *Lasers Surg. Med.* 7:155–159.

Rayleigh, L. 1917. On the pressure developed in a liquid during collapse of a spherical cavity. *Phil. Mag.* 34:94–98.

Ren, Q., V. Venugopalan, K. Schomacker, T. F. Deutsch, T. J. Flotte, C. A. Puliafito, and R. Birngruber. 1992. Mid-infrared laser ablation of the cornea: a comparative study and its application. *Lasers Surg. Med.* 12:274–281.

Schoeffmann, H., H. Schmidt-Kloiber, and E. Reichel. 1988. Time-resolved investigations of laser-induced shock waves in water by use of polyvinylidenefluoride hydrophones. *J. Appl. Phys.* 63:46–51.

Sigrist, M. W. 1986. Laser generation of acoustic waves in liquids and gases. *J. Appl. Phys.* 60:R83–R121.

Skripov, V. P. 1974. Metastable Liquids. John Wiley and Sons, New York.

Smith, L. T., K. A. Holbrook, and P. H. Byers. 1982. Structure of the dermal matrix during development and in the adult. *J. Invest. Dermatol.* 79:93s–104s.

Srinivasan, R. 1986. Ablation of polymers and biological tissue by ultraviolet lasers. *Science.* 234:559–565.

Srinivasan, R., P. E. Dyer, and B. Braren. 1987. Far-ultraviolet laser ablation of the cornea: photoacoustic studies. *Lasers Surg. Med.* 6:514–519.

Venugopalan, V. 1994. The thermodynamic response of polymers and biological tissues to pulsed laser irradiation. Sc.D. thesis. Massachusetts Institute of Technology, Cambridge, MA.

Venugopalan, V., N. S. Nishioka, and B. B. Mikić. 1991. Effect of CO_2 laser pulse repetition rate on mass removal and thermal damage in biological tissue. *IEEE Trans. Biomed. Eng.* 38:1049–1052.

Venugopalan, V., N. S. Nishioka, and B. B. Mikić. 1995. The thermodynamic response of soft biological tissues to pulsed ultraviolet laser irradiation. *Biophys. J.* 69:1259–1271.

Verdaasdonk, R. M., C. Borst, and M. J. C. van Gemert. 1990. Explosive onset of continuous wave laser tissue ablation. *Phys. Med. Biol.* 35: 1129–1144.

Vodopyanov, K. L. 1991. Saturation studies of H_2O and HDO near 3400 cm^{-1} using intense picosecond laser pulses. *J. Chem. Phys.* 94: 5389–5393.

Walsh, J. T., Jr., and J. P. Cummings. 1994. Effect of the dynamic optical properties of water on midinfrared laser ablation. *Lasers Surg. Med.* 15:295–305.

Walsh, J. T., Jr., and T. F. Deutsch. 1988. Pulsed CO_2 laser tissue ablation: measurement of the ablation rate. *Lasers Surg. Med.* 8:264–275.

Walsh, J. T., Jr., and T. F. Deutsch. 1989. Er:YAG laser ablation of tissue: measurement of ablation rates. *Lasers Surg. Med.* 9:327–337.

Walsh, J. T., Jr., and T. F. Deutsch. 1991. Measurement of Er:YAG laser ablation plume dynamics. *Appl. Phys. B.* 52:217–224.

Walsh, J. T., Jr., T. J. Flotte, R. R. Anderson, and T. F. Deutsch. 1988. Pulsed CO_2 laser tissue ablation: effect of tissue type and pulse duration on thermal damage. *Lasers Surg. Med.* 8:108–118.

Walsh, J. T., Jr., T. J. Flotte, and T. F. Deutsch. 1989. Er:YAG laser ablation of tissue: effect of pulse duration and tissue type on thermal damage. *Lasers Surg. Med.* 9:314–326.

Walsh, J. T., Jr., and P. T. Staveteig. 1995. Effect of hydrogen bonding on the far-ultraviolet water absorption and potential implications for 193-nm ArF excimer laser-tissue interaction. *Proc. SPIE.* 2391: 176–183.

Weast, R. C., ed. 1985. CRC Handbook of Chemistry and Physics. CRC Press, Boca Raton, FL.

Wolbarsht, M. 1984. Laser surgery: CO_2 or HF. *IEEE J. Quantum Elec.* 20:1427–1432.

Yannas, I. V. 1972. Collagen and gelatin in the solid state. *J. Macromol. Sci. Revs. Macromol. Chem.* C7:49–104.

Zweig, A. D. 1991a. Infrared laser ablation: consequences of liquefaction. *Proc. SPIE.* 1427:2–8.

Zweig, A. D. 1991b. A thermo-mechanical model for laser ablation. *J. Appl. Phys.* 70:1684–1691.

Zweig, A. D., V. Venugopalan, and T. F. Deutsch. 1993. Stress generated in polyimide by excimer-laser irradiation. *J. Appl. Phys.* 74:4181–4189.

Zweig, A. D., and H. P. Weber. 1987. Mechanical and thermal parameters in pulsed laser cutting of tissue. *IEEE J. Quantum Elec.* 23:1787–1793.